American Mineralogist, Volume 59, pages 563–566, 1974

The Spectrum of Fe^{2+} Ions in Silicate Garnets

W. Alan Runciman, and Dipankar Sengupta

Department of Solid State Physics, Research School of Physical Sciences, Australian National University, Canberra, A.C.T. 2600 Australia

Abstract

The recent interpretation of the three intense near-infrared bands of Fe^{2+} in silicate garnets by White and Moore (1972) is re-examined using a point charge model. The inclusion of second nearest neighbor silicon atoms in the calculation leads to substantial modification of the level assignments. The bands at 4500, 6100, and 7800 cm^{-1} are now assigned to transitions from the $d_{z^2}(A)$ orbital ground state to $d_{xy}(B_1)$, $d_{zx}(B_2)$ and $d_{yz}(B_3)$ orbitals respectively. The present assignments are also consistent with the selection rule requirement that the $d_{z^2}(A) \rightarrow d_{x^2-y^2}(A)$ transition is forbidden.

Introduction

The electronic spectra of Fe^{2+} in silicate garnets have recently been discussed by Burns (1969, 1970) and by White and Moore (1972). The Fe^{2+} ions occupy the 8-fold site in garnet that has an exact D_2 symmetry. Three strong bands in the infrared region of the garnet spectrum have been assigned to the spin-allowed transitions of Fe^{2+}. Since the garnet crystals are cubic, no polarization data are available. This makes the task of symmetry assignment of the energy levels rather difficult. White and Moore (1972) tackled this difficulty by considering qualitatively the effect of nearest neighbor oxygen ions on the different *d*-orbitals. Based on this model, they had to assign the 4500 cm^{-1} band to the $A(d_{z^2}) \rightarrow A(d_{x^2-y^2})$ transition. This transition is forbidden according to the group theoretical selection rules. A quantitative calculation was performed by the present authors using a point charge model as outlined in Garner and Mabbs (1970). When the nearest neighbor oxygen ions are considered, the energy level scheme proposed by White and Moore is reproduced. However, the inclusion of next nearest neighbor silicon atoms in the calculation produced a significant change from the energy levels proposed by White and Moore, and led to a level assignment consistent with the selection rules. The methods of this paper are similar to those used for enstatite (Runciman, Sengupta, and Marshall, 1973) and for olivine (Runciman, Sengupta, and Gourley, 1973).

Experimental

A number of pyrope-almandine garnets have been studied. The spectrum shown in Figure 1 is from a pyrope garnet of the following composition: pyrope 59.1 percent, almandine 28.6 percent, grossularite 11.6 percent, and spessartite 0.7 percent with the physical properties sp gr = 3.75, a_o = 11.51 Å. The spectrum, recorded at liquid helium temperature using a Cary 17 spectrophotometer, shows three strong infrared bands—at 4500, 6110, and 7830 cm^{-1}—whose positions and temperature dependence are consistent with the results of White and Moore (1972) and of Manning (1967). The far infrared region below 2000 cm^{-1} of the spectrum is dominated by strong lattice vibrational bands. A number of bands are also observed in the visible region and are probably due to spin-forbidden transitions. Moore and White (1972) discuss these bands for 19 selected garnets.

Crystallographic Data

The crystal-chemical and crystallographic data for a series of garnets have been collected by Novak and Gibbs (1971). The results for pyrope garnet given in that paper have been used for the present computation. The descent-of-symmetry for the 8-fold site from O_h to D_2 has been adequately discussed by White and Moore (1972). Figure 2 shows the projection of the coordination polyhedron consisting of nearest neighbor oxygens on the plane normal to the pseudo-fourfold axis. Two silicon atoms located ± 2.88 Å away from the metal ion along the *x* axis are also shown in the figure. This projection makes it easier to visualize the distortion from a cubic site. This consists of a reduction of distance between the oxygen atoms near the *x* axis (and on the same side of the *y* axis), and a twist of the four top atoms with respect to the lower-layer atoms.

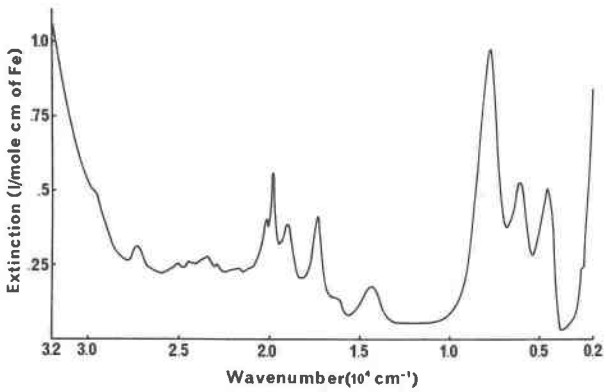

FIG. 1. Absorption spectrum of a pyrope garnet at 15 K over the wavelength range 2000–32000 cm^{-1}.

Point Charge Model

The eight nearest-neighbor oxygen ions may be classified into sets of four, labelled A and B. The set of four oxygens with z-coordinates of $\pm$ 1.19 Å are A ions and the remaining four are B ions. The total crystal field potential exerted by these sets of ligands and the two next-nearest-neighbor silicon atoms, considered as point charges, is readily obtained. The matrix elements between the single electron d-functions under the action of this potential are given in the appendix. The parameters used are $Dq = Ze^2\langle r^4\rangle/6R_A{}^5$ and $Cp = 2Ze^2\langle r^2\rangle/7R_A{}^3$ where R_A represents the shortest metal-ligand distance and Ze is the charge on the oxygen ions. The charge on the silicon ions is taken to be -2 Ze. The Dq and Cp values for more distant oxygen and silicon ions are weighted by appropriate $(R_A/R_i)^5$ and $(R_A/R_i)^3$ factors where R_i is the appropriate metal-oxygen or metal-silicon distance.

Crystal Field Calculations

Initial calculations using the nearest-neighbor oxygen interactions produced an ordering of the orbitals consistent with the qualitative results of White and Moore (1972). This ordering is indicated on the right hand side of Figure 3. The orbitals have the following correspondence: $A = d_{x^2-y^2}$ and d_{z^2}, $B_1 = d_{xy}$, $B_2 = d_{zx}$, $B_3 = d_{yz}$. The A orbitals are mixed, but the ground state is predominantly d_{z^2}, and the upper A state predominantly $d_{x^2-y^2}$. As pointed out earlier, this scheme is not consistent with

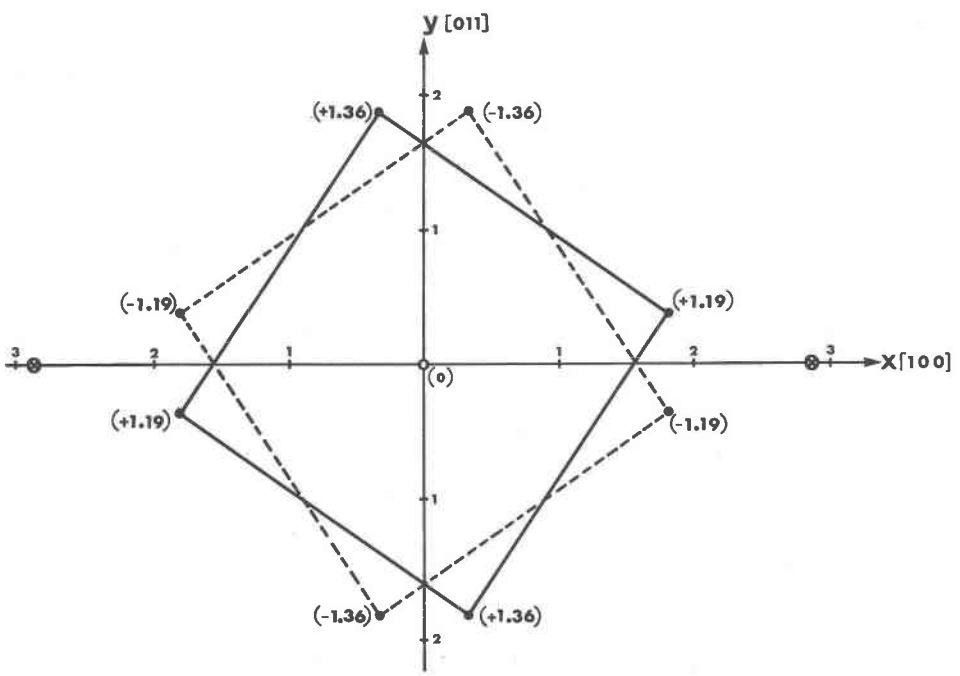

FIG. 2. Projection of the 8-fold oxygen-coordinated site in garnet on the plane normal to the pseudo-fourfold axis. The numbers in the brackets refer to the z-coordinate of the corresponding oxygen atoms. All numbers are in Å units. The Fe^{2+} site is at the origin, and the silicon sites are on the x-axis.

group theoretical selection rules. The selection rules indicate that an $A \rightarrow A$ transition is forbidden, yet according to this scheme the 4500 cm^{-1} band has to be assigned to an $A \rightarrow A$ transition.

By contrast, when contributions from the two nearest silicon ions were included in the calculations, the relative ordering of the orbitals changed drastically as shown on the left side of Figure 3. This new scheme assigns the 4500 cm^{-1} band to an allowed $A \rightarrow B_1$ transition.

The values of the angular parts of the crystal field potential (as defined in the appendix) for these two cases are as follows: $\alpha = -5.02$ (-5.02) $\beta = 0.125$ (-0.125), $\gamma = 0.33$ (0.59), $\delta = 0.34$ (0.09), $\epsilon = -0.31$ (0.13) where the numbers in parentheses correspond to the contributions from nearest neighbor oxygens. Inclusion of the silicons has a maximum effect on the δ and ϵ terms which correspond to the B_4^2 and B_2^2 terms in the usual crystal-field notation. In fact the sign of ϵ is reversed. The physical reason for such a large effect can be understood as follows. When we consider the nearest-neighbor oxygens, the deviation from cubic symmetry is not large, hence the $\delta(B_4^2)$ and $\epsilon(B_2^2)$ terms are small. Putting it in a different way, the contributions to δ and ϵ from the A and B sets of oxygens (oxygen ions along the x and y axes respectively in Figure 2) nearly cancel each other. On the other hand the contributions from the two silicon ions along the x axis add up.

The Dq and Cp values were obtained by fitting B_2 and B_3 levels to the 6100 and 7800 cm^{-1} bands respectively. The values obtained were $Dq = 780$ cm^{-1} and $Cp = 1710$ cm^{-1}. These Dq and Cp values were then used to predict the positions of the $A(d_{x^2-y^2})$ and $B_1(d_{xy})$ levels. The predicted positions are 3500 and 7100 cm^{-1} for the B_1 and A levels respectively. On the basis of this calculation the lowest observed band has been assigned to the B_1 state.

The energy matrix presented in the appendix shows that the energy difference between the B_2 and B_3 levels is due to contributions from the $\delta(B_4^2)$ and $\epsilon(B_2^2)$ terms. On the other hand the A to B_1 splitting is mainly due to the $\beta(B_2^0)$ and $\gamma(B_4^4)$ terms, the δ and ϵ terms occurring as off-diagonal elements. It has been asserted in the last section that the silicon atoms add major contributions to the δ and ϵ terms. This makes one wonder why the $B_2 \leftrightarrow B_3$ splitting is not much larger compared to $A \leftrightarrow B_1$ splitting. The reason for the small $B_2 \leftrightarrow B_3$ splitting is that δ and ϵ have opposite signs and their contributions partially cancel each other. In fact, the ϵ term has gone to such a high negative value that it has resulted in a reversal of position between B_2 and B_3 compared to the earlier assignment.

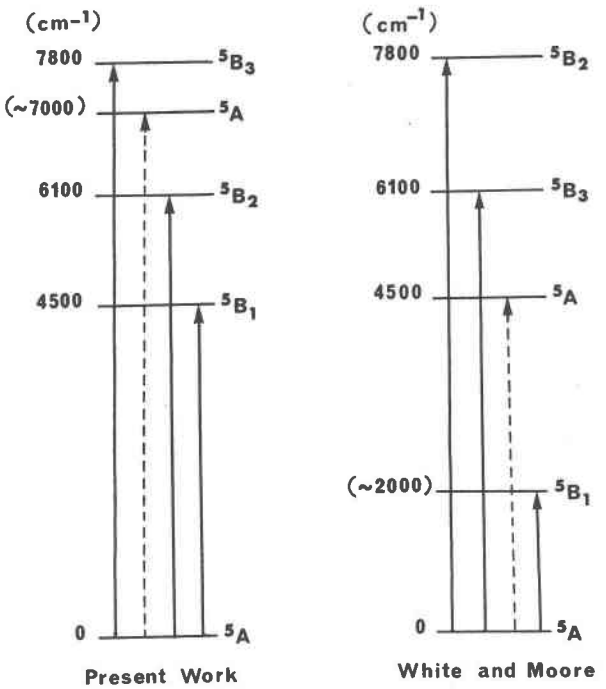

FIG. 3. The energy level scheme for Fe^{2+} levels in garnet. The dashed arrows indicate the forbidden transitions. The numbers in brackets correspond to the levels not observed experimentally.

Conclusions

A crystal-field calculation based on a point charge model that includes the effects of nearest-neighbor oxygen and silicon atoms yields symmetry assignments consistent with the selection rules. Although the predicted ordering of the levels is probably correct, the numbers given for the parameters and energy levels are only approximate. The model is limited by the fact that it ignores the interaction with the rest of the structure. Secondly, the point charge description is definitely inadequate for the silicon atoms which are expected to be covalently bonded to the nearest oxygen atoms.

A spin-orbit calculation for $\zeta = 400$ cm^{-1} was performed with the hope that a future electron spin-resonance experiment would put the model on a more quantitative basis. The spin-orbit components for the ^5A ground state were calculated to be at 0, 0.02, 13.1, 13.7, 17.9 cm^{-1}.

Acknowledgments

The authors are grateful to the Research School of Earth Sciences, A.N.U., for performing the microprobe analysis on the garnet sample, and to Mr. M. Marshall for taking the optical spectra.

Appendix

The crystallographic data used for pyrope garnet are as follows:

	R(Å)	θ(degree)	ϕ(degree)
(A) Oxygen (1)	2.20	57°	12°
(B) Oxygen (2)	2.34	55°	80°
(C) Silicon	2.88	90°	0°

where R is the metal-oxygen or metal-silicon distance; θ and ϕ are defined with respect to the coordinate axes shown in Figure 2. The energy levels in terms of the Dq and Cp parameters defined in the text are as follows:

$$E_{d_{yz}}(B_3) = Dq\left(-\frac{4\alpha}{7} - \frac{20\delta}{7}\right) + Cp(\beta - 3\epsilon)$$

$$E_{d_{xz}}(B_2) = Dq\left(-\frac{4\alpha}{7} + \frac{20\delta}{7}\right) + Cp(\beta + 3\epsilon)$$

$$E_{d_{xy}}(B_1) = Dq\left(\frac{\alpha}{7} - 5\gamma\right) - 2Cp\beta$$

and the two A energy levels are found by solving the matrix equation:

$$\begin{vmatrix} \frac{6\ Dq\alpha}{7} + 2Cp\beta - \lambda & \frac{10\sqrt{3}}{7}\ Dq\delta - 2\sqrt{3}\ Cp\epsilon \\ \frac{10\sqrt{3}}{7}\ Dq\delta - 2\sqrt{3}\ Cp\epsilon & Dq\left(\frac{\alpha}{7} + 5\gamma\right) - 2Cp\beta - \lambda \end{vmatrix} = 0$$

where

$$\alpha = (35\cos^4\theta_A - 30\cos^2\theta_A + 3) + \left(\frac{R_A}{R_B}\right)^5(35\cos^4\theta_B - 30\cos^2\theta_B + 3) - \left(\frac{R_A}{R_C}\right)^5(35\cos^4\theta_C - 30\cos^2\theta_C + 3),$$

$$\beta = (3\cos^2\theta_A - 1) + \left(\frac{R_A}{R_B}\right)^3(3\cos^2\theta_B - 1) - \left(\frac{R_A}{R_C}\right)^3(3\cos^2\theta_C - 1),$$

$$\gamma = \sin^4\theta_A\cos 4\phi_A + \left(\frac{R_A}{R_B}\right)^5\sin^4\theta_B\cos 4\phi_B - \left(\frac{R_A}{R_C}\right)^5\sin^4\theta_C\cos 4\phi_C,$$

$$\delta = \sin^2\theta_A(7\cos^2\theta_A - 1)\cos 2\phi_A + \left(\frac{R_A}{R_B}\right)^5\sin^2\theta_B(7\cos^2\theta_B - 1)\cos 2\phi_B - \left(\frac{R_A}{R_C}\right)^5\sin^2\theta_C(7\cos^2\theta_C - 1)\cos 2\phi_C,$$

$$\epsilon = \sin^2\theta_A\cos 2\phi_A + \left(\frac{R_A}{R_B}\right)^3\sin^2\theta_B\cos 2\phi_B - \left(\frac{R_A}{R_C}\right)^3\sin^2\theta_C\cos 2\phi_C.$$

A and B refer to two sets of oxygen atoms defined in the text, and C refers to the two silicon atoms.

If the crystal field potential is expressed as $\Sigma B_k^q C_k^q$ where $C_k^q = [4\pi/(2k+1)]^{1/2}Y_k^q$, then B_k^q can be defined in terms of Dq and Cp as follows:

$$B_2^0 = 7\ Cp\beta, \qquad B_2^2 = 7\sqrt{\frac{3}{2}}\ Cp\epsilon, \qquad B_4^0 = 3\ Dq\alpha$$

$$B_4^4 = \frac{5\times 21}{\sqrt{70}}\ Dq\gamma, \qquad B_4^2 = 3\sqrt{10}\ Dq\delta.$$

References

BURNS, R. G. (1969) Optical absorption in silicates. In, S. K. Runcorn, Ed., *The Application of Modern Physics to the Earth and Planetary Interiors.* John Wiley and Sons, New York.

——— (1970) *Mineralogical Applications of Crystal Field Theory.* Cambridge University Press, Cambridge.

GARNER, C. D., AND F. E. MABBS (1970) Studies in eight coordination. Part I. Crystal field energies in the D_{2d} point group. *J. Chem. Soc.* **(A),** 1711–1716.

MANNING, P. G. (1967) The optical absorption spectra of the garnets almandine-pyrope and spessartine and some structural interpretations of mineralogical significance. *Can. Mineral.* **9,** 237–251.

MOORE, R. K., AND W. B. WHITE (1972) Electronic spectra of transition metal ions in silicate garnets. *Can. Mineral.* **11,** 791–811.

NOVAK, G. A., AND G. V. GIBBS (1971) The crystal chemistry of the silicate garnets. *Am. Mineral.* **56,** 791–825.

RUNCIMAN, W. A., D. SENGUPTA, AND J. T. GOURLEY (1973) The polarized spectra of iron in silicates. II. Olivine. *Am. Mineral.* **58,** 451–456.

———, ———, AND M. MARSHALL (1973) The polarized spectra of iron in silicates. I. Enstatite. *Am. Mineral.* **58,** 444–450.

WHITE, W. B., AND R. K. MOORE (1972) Interpretation of the spin-allowed bands of Fe^{2+} in silicate garnets. *Am. Mineral.* **57,** 1692–1710.

Manuscript received, October 9, 1973; accepted for publication, October 24, 1973.